SYNTHESIS CHARACTERIZATION AND MAGNETIC STUDIES OF MANGANESE SUBSTITUTED MgCo$_2$O$_4$ SYNTHESIZED BY SOL-GEL METHOD

A. V. Mali

UG and PG Department of Chemistry,

Yashwantrao Chavan College of Science, Karad. Maharashtra. India- 415124

Corresponding author E-mail: ankushvmali@gmail.com

ABSTRACT:

Powder Mg$_{(1-x)}$Mn$_x$Co$_2$O$_4$ (where x=0.0, 0.25, 0.50, 0.75 and 1.0) samples were prepared by sol-gel technique followed by thermal treatment. The structural and magnetic properties of the samples has been investigated by different techniques. All samples were cubic with a spinel structure shown by x-ray diffraction patterns. Diffraction lines were broadened indicating nanocrystalline samples. The magnetic character increase with increas in Mn contain while Magnesium interfere in magnetic properties of the system.

KEYWORDS: Sol-gel method, characterization, magnetic.

INTRODUCTION:

Mixed metal oxide nanoparticles are technologically important for their wide areas of application such as electrodes in solar cells [1], lithium ion batteries [2],

electrochemical capacitors [3], in molten carbonate fuel cells [4], electro-catalysts [5], optical limiters and switches [6] and chemical sensors [7] etc. Especially, their role in magnetic material [8-11]. One of the most attractive features on metal oxide materials is the magneto electric coupling for which both order parameters (magnetic and electric) are directly coupled [12]. Among these materials, the magnetic oxides crystallizing in the perovskite ABO_3 and spinelAB_2O_4 structures (A and B, cationic positions) are especially interesting because their structural, electronic and magnetic properties can be easily modified by slightly doping their crystal structures [13-14].

The first application of magnetite (ferrite) was as 'Lodestones' used by early navigators to locate magnetic North [15]. This material has been expansively premeditated by number of researchers. Masahiko Sato made the saturation magnetization measurements of magnetite [16]. The magnetic properties such as saturation magnetization and Curie temperature were studied by Jing Wang [17]. These effects can be obtained by changing the chemical composition and the cation distribution in the perovskite and spinel structures [18].

In this work, we have specially investigated the structure of $Mg_{(1-x)}Mn_xCo_2O_4$ and effect of manganese on the structural and magnetic properties of manganese substituted magnesium cobaltite.

EXPERIMENTAL:

Manganese substituted magnesium cobaltite $Mg_{(1-x)}Mn_xCo_2O_4$ (where x=0.0, 0.25, 0.50, 0.75 and 1.0) samples were prepared by sol-gel auto combustion method [19]. The A.R. Grade chemicals used in the synthesis of materials were $C_6H_8O_7.2H_2O$, $Mg(NO_3)_2.6H_2O$, $Mn(No_3)_2.4H_2O$, $Co(NO_3)$ H_2O and NH_3. The metal nitrates were dissolved in deionised water and equal quantities of citric acid were added in the metal nitrate solution. In beaker citrate solutions of Manganese nitrate, magnesium

nitrate and cobalt nitrate were mixed in required stoichiometric ratio. The ammonia solution (1:1) was added drop by drop until the pH of the solution reached a value of 9.5. The resulting solution was stirred for 3h to maintain the homogeneity. The gel is formed when solution were heated on hot plate at 100°C after words the gel is further heated at 150°C to convert into fluphy mass. This fluphy mass was annealed at the temperature of 600°C for 6 h in a Box furnace.

In order to investigate the grain size and phase X-ray diffraction (XRD) analysis was performed (Philips PW-1710 X-ray diffractometer with CuKα radiation).

RESULTS AND DISCUSSION:

XRD analysis:

Powder X-ray diffraction (XRD) was utilized to purity and characterize the phase of prepared $Mg_{(1-x)}Mn_xCo_2O_4$ as shown in Fig.1. XRD pattern shows the characteristic peaks at 31.3°, 36.9°, 44.8°, 55.7°, 59.4° and 65.3° according to JCPDS Card No. 23-1237, which can be indexed to (220), (311), (400), (422), (511) and (440) planes of the cubic spinel with Fd3m space group. The sharp peaks observed in the XRD pattern demonstrate a crystalline phase of the samples. Average crystallite size has been calculated from the full width at half-maximum (FWHM) in the 311 reflection peak applying the Scherrer equation [20].

$$D = \frac{0.9\lambda}{\beta\cos\theta}$$

Where λ is the incident wavelength of Cu Kα radiation of the XRD, β is the peak width at mid-height and θ is the considered angle. The crystallite size increases with increase in manganese contents. The average crystallite size of the synthesized powders lies in-between 34.41 to 25.14nm. For $MgCo_2O_4$ (Fig.1), where Mn is completely substituted by Mg^{2+} ions, assuming a standard spinel structure (JCPDS

Card no. 23-1237). The value of lattice constant 'a' of the $MgCo_2O_4$ spinel as calculated from XRD data is 8.197 Å. The lattice constant 'a' increases on increasing the Mn^{2+} concentration in material as shown in table 1. The increase in lattice constant is due to the fact that the ionic radius of Mg^{2+} (0.65 Å) is smaller than that of Mn^{2+} (0.80 Å). The increase in 'a' on increasing the concentration of Mn^{2+} ions demonstrates that the Mn^{2+} ions actually enter the crystal lattice and retain the cubic spinel structure. The X-ray densities for all samples were calculated using the relation [21].

$$dx = \frac{8M}{Na^3}$$

Where, N = Avogadro's number (6.023×10^{23} atom/mole)

M = Molecular weight.

a = lattice constant.

The increase in the dx is considered to be due to the fact that the atomic mass of Mn^{2+} is larger than that of Mg^{2+}. The lattice parameters of $Mg_{(1-x)}Mn_xCo_2O_4$ were found to 8.197 to 8.238 Å.

Fig.1. XRD patterns of the system $Mg_{1-x}Mn_xCo_2O_4$.
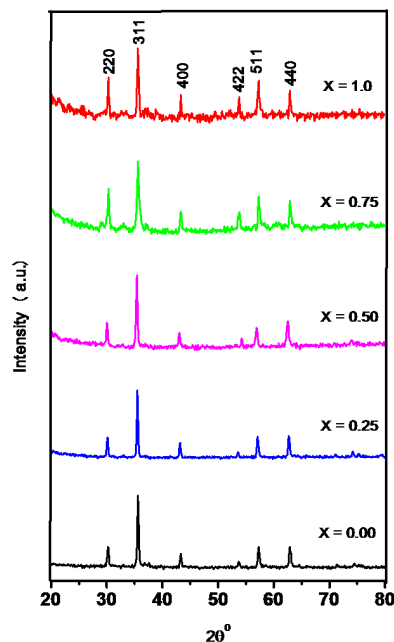
Table 1. Lattice constant, Crystallite size, and X-ray density of the system $Mg_{1-x}Mn_xCo_2O_4$:

1.1.1.1. Composition	1.1.1.2. Lattice 1.1.1.3. Constants (Å)	1.1.1.4. Crystallite 1.1.1.5. Size (nm)	1.1.1.6. X-ray density 1.1.1.7. (dx) (gm/cm^3)
1.1.1.8. x = 0.0	1.1.1.9. 8.197	1.1.1.10. 34.41	1.1.1.11. 3.72
1.1.1.12. x = 0.25	1.1.1.13. 8.214	1.1.1.14. 34.46	1.1.1.15. 3.87
1.1.1.16. x = 0.50	1.1.1.17. 8.221	1.1.1.18. 34.62	1.1.1.19. 3.89
1.1.1.20. x= 0.75	1.1.1.21. 8.227	1.1.1.22. 34.93	1.1.1.23. 4.12
1.1.1.24. x = 1.0	1.1.1.25. 8.238	1.1.1.26. 35.14	1.1.1.27. 4.27

Magnetic Properties:

The plots of magnetization (M) as a function of applied magnetic field (H) are shown in Fig.2. (a-c) of the system $Mg_{(1-x)}Mn_xCo_2O_4$, obtained at room temperature. Lists of different parameters like coercive force (Hc), saturation magnetization (Ms), remnant magnetization (Mr) and magnetic moment (μβ) are given in table 2. The magnetic properties are changed by the substitution of Mn^{2+} content. It was observed that all this compound produce a very narrow hysteresis loops, which indicates behavior characteristics of soft magnetic materials. Shape and width of hysteresis cycle depend on a number of factors such as synthesis technique, chemical

composition and redistribution of cations between the tetrahedral and octahedral sites [22]. The Mg^{2+} and Mn^{2+} has preference to occupy tetrahedral A site and CO^{3+} ions are preferentially occupy to octahedral B site. Due to magnetic substitution of Mn ions at tetrahedral A site magnetic moment increases. The magneton number ($\mu\beta$) is calculated from the hysteresis data by using the relation.

$$M\beta = \frac{\text{Molecular weight X Saturation Magnetization}}{5585}$$

(a)

(b)

(c)
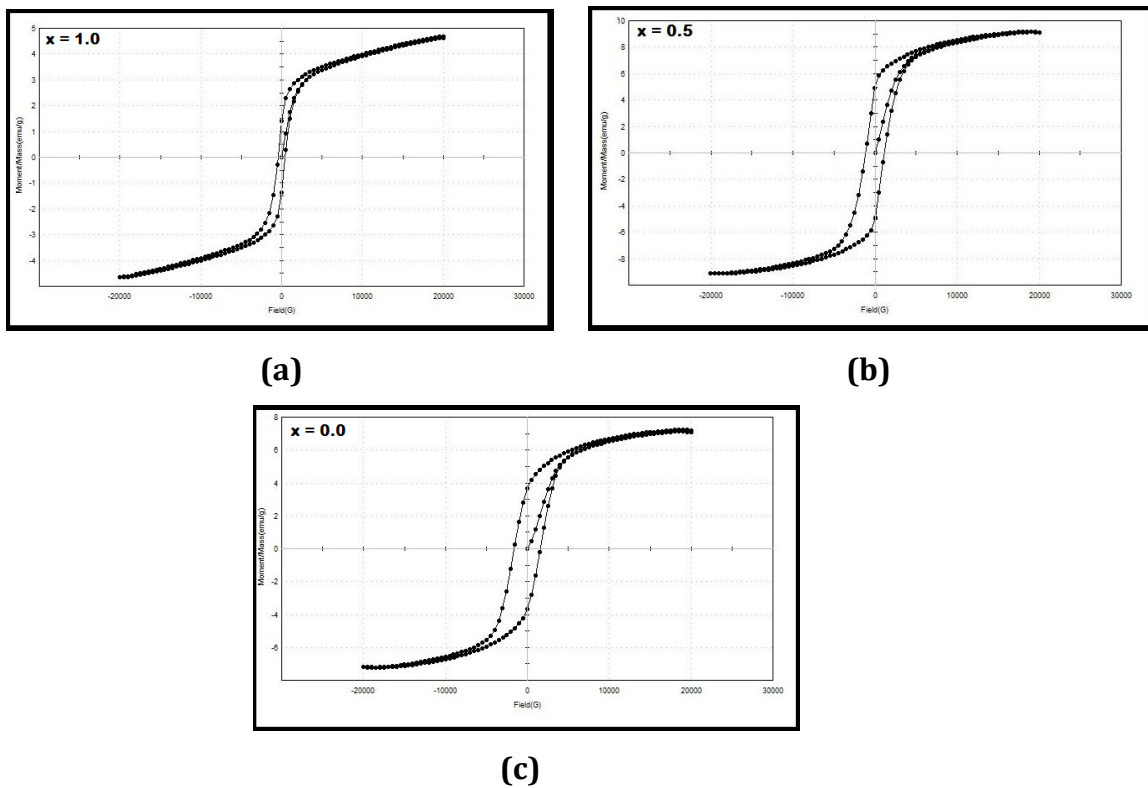
Fig. 2. Hysteresis loop of the system $Mg_{1-x}Mn_xCo_2O_4$ (a, x = 0.0, b, x = 0.5 and c, x = 1.0)

Table 2. Coercivity (Hc), Saturation Magnetisation (Ms), Retentivity (Mr) and Magnetic moment of the system $Mg_{1-x}Mn_xCo_2O_4$

1.1.1.28. Composition	1.1.1.29. Coercivity (Hc)	1.1.1.30. Saturation Magnetisation (Ms)	1.1.1.31. Remenant magnetization (Mr)	1.1.1.32. Magnetic moment
1.1.1.33. x = 0.0	1.1.1.34. 79.92	1.1.1.35. 6.79	1.1.1.36. 38.47	1.1.1.37. 0.25
1.1.1.38. x = 0.5	1.1.1.39. 39.92	1.1.1.40. 11.35	1.1.1.41. 36.25	1.1.1.42. 0.45
1.1.1.43. x = 1.0	1.1.1.44. 217.26	1.1.1.45. 46.42	1.1.1.46. 4.78	1.1.1.47. 1.96

CONCLUSION:

The structural and magnetic properties of manganese substituted manganese cobaltite have been investigated. The sol-gel autocombution method is successfully used for the synthesis of manganese substituted $MgCo_2O_4$, where Mg^{+2} ions are completely replaced by Mn^{+2} ions, is found to be spinel structure. The result obtained by XRD pattern dictate that the lattice constant, bulk density and X-ray density are affected by the Mn^{+2} substitution. The particle size is found to be 37 nm. The magnetic character increase with increase in Manganese contain, while Magnesium interfere in magnetic properties of the system.

REFERENCES:

[1] Kuznetsov I.A., Greenfield M.J., Mehta Y.U., Merchan-Merchan, Salkar G., Saveliev A. V.: Increasing the solar cell power output by coating with transition metal-oxide nanorods. Applied Energy. 88, 4218–4221 (2011).

[2] Sharma Y., Sharma N., Rao G.V.S., Chowdari B.V.R.: Studies on spinel cobaltites, $FeCo_2O_4$ and $MgCo_2O_4$ as anodes for Li-ion batteries. Solid State Ionics 179, 587–597 (2008).

[3] Lu Q., Chen Y., Li W., Chen J.G., Xiao J.Q., Jiao F.: Ordered mesoporous nickel cobaltite spinel with ultra-high supercapacitance. J. Mater. Chem. A 1, 2331–2336 (2013).

[4] Fukui T., Okawa H., Hotta T., Naito M.: Synthesis of CoO/Ni Composite Powders for Molten Carbonate Fuel Cells. J. Am. Ceram. Soc. 84 (1), 233–235 (2001).

[5] Yang J., Xu J.J.: Nanoporous amorphous manganese oxide as electrocatalyst for oxygen reduction in alkaline solutions. Electrochemistry Communications. 5, 306–311 (2003).

[6] Windisch Jr., Exarhos G.J., Ferris K.F., Engelhard M.H., Stewart D.C.: Infrared transparent spinel films with p-type conductivity. Thin Solid Films. 398, 45–52 (2001).

[7] Khan S.B., Rahman M.M., Akhtar K., Asiri A.M., Alamry K.A., Seo J., Han H.: Copper Oxide Based Polymer Nanohybrid for Chemical Sensor Applications. Int. J. Electrochem. Sci. 7, 10965–10975 (2012).

[8] Moritomo Y., Asamitsu A., Kuwahara H., Tokura Y.: Giant magnetoresistance of manganese oxide with a layered pervoskite structure, Nature 380, 141–144 (1996).

[9] Ichiyanagi, Y., Kubota, M., Moritake, S., Kanazawa, Y., Yamada,T., Uehashi, T.: J. Magn. Magn. Mater. **310**, 2378–2380 (2007)

[10] Zein K. Heiba, Mohamed Bakr Mohamed, Adel MaherWahba, Arda L.: Magnetic and Structural Properties of Nanocrystalline Cobalt-Substituted Magnesium–Manganese Ferrite. J Supercond Nov Magn. 28, 2517–2524 (2015).

[11] Kaewrawang, A., Ghasemi, A., Liu, X., Morisako, A.: Crystallographic and magnetic properties of SrM thin films on Pt under layer prepared at various substrate temperatures. J. Magn. Magn. Mater. **321**, 1939–1942 (2009)

[12] Lassri1 M., Elamiri A., Chafai K., Abid M., Hlil E. K., MoubahR., Lassri H.: Investigation of Magnetic and Electronic Properties of Sputtered Fe/Au Multilayers. J Supercond Nov Magn. (January 2016) DOI 10.1007/s10948-016-3427-0

[13] Elahmar M.H., Rached H., Rached D., Khenata R., Murtaza G., Bin Omran S., Ahmed W.K.: Structural, mechanical, electronic and magnetic properties of a new series of quaternary Heusler alloys CoFeMnZ (Z=Si, As, Sb). Journal of Magnetism and Magnetic Materi 393, 165-174 (2015)

[14] Talik E., Lipinska L., Zajde P. Zalog , A., Michalska M., Guzik A.:Electronic structure and magnetic properties of $LiMn_{1.5}M_{0.5}O_4$ (M=Al, Mg, Ni, Fe) and $LiMn_2O_4/TiO_2$ nanocrystalline electrode materials. Journal of Solid State Chemistry, 206, 257-264 (2013).

[15] Joris Fellinger, Konstantin Egorov, Victor Bykov, Felix Schauer.: Preparation for commissioning of structural sensors of Wendelstein 7-X magnet system. Fusion Engineering and Design, 98, 1048-1052 (2015).

[16] Masahiko Sato, Yuhji Yamamoto, Takashi Nishioka, Kazuto Kodama, Nobutatsu Mochizuki, Hideo Tsunakawa.: Hydrostatic pressure effect on magnetic hysteresis parameters of multidomain magnetite: Implication for crustal magnetization. Physics of the Earth and Planetary Interiors, 233, 33-40 (2014).

[17] Jing Wang, Lin-Jie Dai, Chang-Min Xiong, Xuan Zhao, Ning Wang, Wei-Jian Lou,

Tianxing Ma.: Dependence of the magnetism–resistivity correlation on Curie temperature in manganites. Solid State Communications, 181, 28-33 (2014).

[18] *Souiri M., Goltzene A., Schwab C.:Criteria for preferential extrinsic cation location in the structures of the perovskite and spinel groups, Progress in Crystal Growth and Characterization. 10, 27-30 (1984).*

[19] Mali A. V., Wandre T. M., Sanadi K. R. , Tapase A. S., Mulla I. S., Hankare P. P..: Synthesis, characterization and electrical properties of novel Mn substituted $MgAl_2O_4$ synthesized by sol–gel method. J. Mater. Sci. Mater. Electron. (2015) doi 10.1007/s10854-015-3796-3.

[20] Yashpal, Vipin Sharma, B.V. Manoj Kumar.: Issues in Determining Size of Nano-crystalline Ceramic Particles by X-ray Diffraction, Materials Today: Proceedings, 2, Issues 4–5 (2015) 3534-3538.

[21] Fei Cai, Chuanhai Jiang, Xueyan Wu.:X-ray diffraction characterization of electrodeposited Ni–Al composite coatings prepared at different current densities, Journal of Alloys and Compounds, 604, 292-297 (2014).

[22] *Sattar, H.M. EL-Sayed, Ibrahim ALsuqia.:Structural and magnetic properties of $CoFe_2O_4/NiFe_2O_4$ core/shell nanocomposite prepared by the hydrothermal method, Journal of Magnetism and Magnetic Materials, 395, 89-96.A.A, (2015).*